Testing the minimum thermal conductivity model for amorphous polymers using high pressure

Wen-Pin Hsieh, Mark D. Losego, Paul V. Braun, Sergei Shenogin, Pawel Keblinski, and David G. Cahill

Testing the minimum thermal conductivity model

for amorphous polymers using high pressure

Wen-Pin Hsieh, [1,2,]* Mark D. Losego,[3] Paul V. Braun,[2,3] Sergei Shenogin,[4] Pawel

Keblinski,[4] and David G. Cahill[2,3]

[1]*Department of Physics, University of Illinois, Urbana, Illinois 61801, USA*

[2]*Frederick-Seitz Materials Research Laboratory, University of Illinois, Urbana, Illinois*

61801, USA

[3]*Department of Materials Science and Engineering, University of Illinois, Urbana,*

Illinois 61801, USA

[4]*Department of Materials Science and Engineering, Rensselaer Polytechnic Institute,*

Troy, New York 12180, USA

Pressure dependence of thermal conductivity provides a critical test of the validity of the

model of the minimum thermal conductivity for describing heat transport by molecular

vibrations of an amorphous polymer. We measure the pressure dependence of the thermal

conductivity $\Lambda(P)$ of poly(methyl methacrylate) (PMMA) using a combination of

time-domain thermoreflectance and SiC anvil cell techniques. We also determine $\Lambda(P)$

from a computational model of amorphous polystyrene. In both cases, $\Lambda(P)$ is accurately

predicted by the minimum thermal conductivity model via the pressure dependence of the

elastic constants and density.

I.   INTRODUCTION

The model of the minimum thermal conductivity was originally proposed by Einstein

[1, 2] who supposed that thermal energy is transported by harmonic interactions between

vibrating atoms with random phases. Allen and Feldman [3, 4] provided a more rigorous

foundation for this model using a harmonic Green-Kubo formalism and introduced the

terminology of "locons, diffusons, and propagons" to classify the vibrational modes of

disordered materials and their contributions to thermal transport. Locons are localized

vibrational modes that do not contribute to thermal transport in the harmonic

2

approximation. Propagons are wave-like acoustic vibrations that are analogous to the

phonons of crystalline solids. The largest fraction of vibrational modes, and the dominant

contributors to heat transport, are diffusons, non-propagating, diffusive vibrational modes

of the type envisioned by Einstein. Building on these ideas and the assumption of a

Debye-like density of vibrational states, the thermal conductivity of most amorphous

materials—and many strongly disordered crystals—can be accurately predicted from the

atomic density and elastic constants. (An important exception was observed recently for

amorphous Si [5] deposited by hot-wire chemical vapor deposition where the

experimental thermal conductivity is a factor of 4 larger than predicted.) In the high

temperature limit where all vibrational modes are thermally excited, the predicted

minimum thermal conductivity is $\Lambda_{\min} = 0.40 k_B n^{2/3} \left(v_l + 2v_t \right)$, where n is the atomic

density and v_l and v_t are the longitudinal and transverse speeds of sound, respectively [2].

The validity of this description of the thermal transport for an amorphous polymer can

be questioned, however, because of strong deviations from a Debye-like density of

vibrational states: stiff force constants associated with covalent bonding within the

polymer backbone and side groups coexist with soft force constants associated with

non-bonding interactions between chains. Furthermore, non-bonded interactions between

the chains are significantly non-linear and anharmonic interactions between localized

3

vibrations, of the type invoked in "fracton hopping" models [6], could conceivably

contribute to heat transport. Evidence for the importance of anharmonicity in the thermal

conductivity of amorphous polymers was recently observed in molecular dynamics

simulations of polystyrene [7] and proteins [8, 9]. Pressure tuning of the thermal

conductivity enables a critical test of the minimum thermal conductivity model by

enabling a continuous variation of the atomic density and elastic constants.

   Prior experimental work on the pressure dependence of the thermal conductivity $\Lambda(P)$

of polymers [10-12] extends to only $P \approx 2$ GPa because of limitations of the types of

pressure cells used in the prior work. Modern diamond or SiC anvil cell techniques

[13-15] easily generate the high pressures needed to significantly alter the elastic

constants of a polymer. For example, the pressure dependence of the elastic constant C_{11}

of a typical glassy polymer is on the order of $C_{11} \approx 8$ GPa+$7P$ and, therefore, at P=10 GPa,

C_{11} increases by an order of magnitude to $C_{11} \approx 80$ GPa, comparable to the elastic

constants of Al at ambient conditions. Here, we present our combined experimental and

computational study of the elastic constants and thermal conductivity Λ of glassy

polymers: an experimental study of poly(methyl methacrylate) and a numerical study of a

computer-based model of polystyrene.

4

II. EXPERIMENTAL DETAILS

SiC anvils were etched in 10% HF solutions, rinsed with DI water, and sonicated in chloroform followed by ethanol to remove surface contaminants. The anvils were then treated with a piranha solution (3 H_2SO_4 : 1 H_2O_2 (v/v)) to hydroxylate the surface and facilitate chemical attachment of the radical initiator, (11-(2-bromo-2-methyl)propionyloxy) undecyltrichlorosilane [16]. PMMA brushes were grown from these surfaces by atom-transfer radical polymerization (ATRP) [17]. By term "brush", we are referring to polymer chains covalently bonded to a surface at spacing shorter than the radius of gyration [18]. Copper (I) chloride was used as the ATRP catalyst. The thickness of the brush and molecular weight of the PMMA chains increased with increasing polymerization time. We determined the thickness of the brush by picosecond acoustics measurements and comparisons to a simulation of the acoustics signals based on Ref. [19]. From this film thickness and the molecular weight, we calculated a grafting density of ≈0.6 chains nm^{-2}, indicating sufficient overlap to force the extension of polymer chains into the brush regime [18].

The PMMA brushes were then coated with a thin Al film, ≈80 nm thick, by magnetron sputter deposition to act as an optical transducer for time-domain thermoreflectance measurements. We pressurized the SiC anvil cell by loading with Ar cryogenically or by

loading with H_2O as the pressure medium. (Since Ar is a liquid at $P<1.3$ GPa and

sometimes leaked from the cell, H_2O was used for measurements at $P<1.4$ GPa. At room

temperature and $P>1.3$ GPa, the equilibrium phase of Ar is a hcp crystal [20].) The

pressure was determined by ruby fluorescence [21].

The thermal conductivity Λ of PMMA brushes was measured by comparing

time-domain thermoreflectance (TDTR) [22-24] data obtained at room temperature to

calculations using a thermal model [25] which takes into account heat flow through the

polymer layer and into the SiC substrate as well as heat flow into the pressure medium

[26]. The thermal model contains many parameters—laser spot size, and the thickness,

heat capacity and thermal conductivity of each layer—but the thermal conductivity of the

PMMA brush is the only significant unknown. The PMMA layers are chosen to be thin so

that most of the heat flows into the high thermal conductivity SiC anvil and only a small

fraction of the heat flows into the low thermal conductivity pressure medium;

uncertainties in the thermal properties of the pressure medium propagate to less than 2%

error in the measurements of the thermal conductivity of our thickest, 22 nm, PMMA

layers at 10 GPa.

The thickness of the Al film was determined by picosecond acoustics and our estimates

of the heat capacity of Al at high pressures were described in Ref. [15]. Changes in the

6

PMMA thickness were calculated from the equation of state of PMMA. (Our approach

for determining the equation of state is described below.) Because the PMMA layers are

"thermally thin", the model is not sensitive to the heat capacity of the PMMA brush.

We cannot directly measure the elastic constant of a thin polymer brush and instead

measured the elastic constant C_{11} of a thick (>1μm), spun-cast layer of PMMA by

time-domain Brillouin scattering [15, 27, 28]. For longitudinal modes in a backscattering

geometry, the Brillouin frequency is $f = 2Nv_l / \lambda$, where N is the refractive index, v_l the

longitudinal sound velocity, and λ=785 nm is the laser wavelength. Figure 1(a) shows the

pressure dependence of f.

We determine the equation of state and elastic constant C_{11} by a self-consistent,

iterative approach; the result is plotted in Fig. 1(b). To begin, we use a trial function for

the isothermal bulk modulus B_T=6 GPa+6P and calculate the pressure dependence of the

density $\rho(P)$, index of refraction $N(P)$, and $C_{11}(P)$ from the picosecond acoustics data

using the Lorentz-Lorenz formula $\left(N^2 - 1\right)/\left(\rho\left(N^2 + 2\right)\right) = A$, where A is a constant [15].

(At ambient pressure ρ=1.19 g cm^{-3} and A=0.241.) Assuming a constant Poisson ratio of

1/3, $B_T(P) = \left(\frac{2}{3}\right)C_{11}(P)$. We fit this $B_T(P)$ to a second order polynomial in P and

calculate the pressure dependence of the molecular density n from $B_T = n(dP / dn)_T$. We

iterate the procedure described above until C_{11} and B_T are self-consistent. The final

7

equation of state is $B_T = B_0 + B_1 P + B_2 P^2$, where B_0=6.15 GPa, B_1=7, and B_2=−0.17 GPa^{-1}.

The atomic density n increases by 31% at 5 GPa and 46% at 10 GPa. We have assumed

that under high pressure the amorphous polymer deforms plastically so that the state of

stress is close to hydrostatic. (At low pressures, the yield strength of PMMA is $\tau_y \approx 0.05$

GPa+0.2P [29].)

III. RESULTS AND DISCUSSION

Figure 2 shows $\Lambda(P)$ of PMMA brushes (solid symbols) with different thicknesses;

$\Lambda(P)$ is independent of the thickness h when $h > 6$ nm and increases monotonically with

increasing P. (The uncertainty in the thermal conductivity measurements is ≈10 % and

dominated by uncertainties in the thicknesses of PMMA and Al.) For comparison, we also

measured $\Lambda(P)$ of a 10 nm thick spun-cast PMMA (open diamond) and found the

spun-cast and brush forms of PMMA show the same behavior. Our data at ambient

pressure, ≈0.185 W m^{-1} K^{-1}, are in good agreement with the literature value, ≈0.20 W m^{-1}

K^{-1} (open square) [30, 31]; the weaker pressure dependence at low pressure regime is

similar to that of prior work by Andersson (open circle) [10] whose ambient value, 0.225

W m^{-1} K^{-1}, is ≈10 % higher than the data reported in Refs. [30, 31].

The fact that brushes and spun-cast layers behave similarly is consistent with our

previous study of the thickness dependence of the effective thermal conductivity at

ambient pressure [32]. The dry polymer brushes that we are studying are amorphous and

the chain extension is relatively small; we estimated previously that the brushes are

extended to only 25% of their contour length and that the enhancement of thermal

conductivity created by this extension is not significant compared to the experimental

uncertainties of the data plotted in Fig. 2.

Data sets for 9 and 22 nm thick brushes and the 10 nm thick spun-cast layer include

measurements for both increasing and decreasing pressure. This lack of hysteresis shows

that any structural changes in the PMMA under pressure are reversible.

Our measurements of the thermal conductivity of PMMA layers include the

contribution to the thermal resistance from the bulk of the material as well as the thermal

resistance of the Al/PMMA and PMMA/SiC interfaces. We have not experimentally

determined the series sum of the Al/PMMA and PMMA/SiC interface conductance;

instead, we estimate $G \approx 300$ MW m^{-2} K^{-1} based on our previous study of the thickness

dependence of the effective thermal conductivity of spun-cast PMMA [32]. Using this

estimate, the sum of the Kapitza lengths of Al/PMMA and PMMA/SiC interfaces is small,

$l_K = \Lambda / G \sim 1$ nm, and therefore we do not expect a significant reduction in the effective

thermal conductivity of PMMA due to the finite interfacial thermal conductance even for

our thinnest (6 nm) brushes.

In Fig. 2, we also compare our data for $\Lambda(P)$ with the behavior predicted by the model of the minimum thermal conductivity Λ_{min} [2]. In the high temperature limit, Λ_{min} depends only on n and the sound velocities, $v_l = \sqrt{C_{11}/\rho}$ and $v_t = \sqrt{C_{44}/\rho}$. If we assume that the ratio C_{11}/C_{44} is approximately independent of pressure, the pressure dependence of Λ_{min} simplifies to $\Lambda_{min} = \Lambda_0 n^{1/6} C_{11}^{1/2}$. A fit to the average of our data at ambient pressure $\Lambda = 0.185\ \text{W m}^{-1}\text{K}^{-1}$ gives $\Lambda_0 = 3.25 \times 10^{-11}\ \text{J}^{1/2}\text{m K}^{-1}\text{s}^{-1}$ using $n=4.3\times10^{28}\ \text{m}^{-3}$ and $C_{11}=9.2$ GPa. The dashed line in Fig. 2 shows an evaluation of this expression using the C_{11} derived from our polynomial fit and n determined by the equation of state $B_T = n(dP/dn)_T$ as described above.

The pressure dependence of the thermal conductivity can also be described approximately by a relatively simple function of pressure. In the limit of high pressure, the elastic constant C_{11} is approximately linear in P, and $n^{1/6}$ is essentially constant. As a result, the predicted thermal conductivity can be expressed as $\Lambda = \Lambda_1 + \Lambda_2 P^{1/2}$, where $\Lambda_1 = 0.185\ \text{W m}^{-1}\text{K}^{-1}$ is the thermal conductivity at ambient pressure and $\Lambda_2 \approx 0.11\ \text{W m}^{-1}\text{K}^{-1}$ GPa$^{-1/2}$.

The predicted thermal conductivity based on $\Lambda_{min} = \Lambda_0 n^{1/6} C_{11}^{1/2}$ captures the trends in our data and accurately predicts $\Lambda(P)$ at higher pressures. We note that in the low pressure

regime, P<1 GPa, our data deviate slightly from the prediction but the difference is small

and comparable to the experimental uncertainties. (Andersson's data show a similar

deviation from the model prediction even after picking a new $\Lambda_0 = 3.95 \times 10^{-11} \, \mathrm{J}^{1/2} \, \mathrm{m} \, \mathrm{K}^{-1} \, \mathrm{s}^{-1}$

to fit the data of Ref. [10] at ambient pressure.) The good agreement between our data

and the model prediction over the entire pressure range supports the idea that the

dominant mechanism of thermal transport in glassy polymers is the exchange of thermal

energy between non-propagating vibrational modes [33].

To gain further insight into the mechanism of heat transport in amorphous polymers,

and to evaluate the generality of our findings, we performed molecular dynamics (MD)

simulations on a model of polystyrene (PS); polystyrene is chosen because of a

well-established set of force field parameters for sp^3- and sp^2-hybridized carbon atoms

and hydrogen atoms existing in Polymer Consistent Force Field [34]. Recently, Algaer

and collaborators [35] also reported the pressure dependence of the thermal conductivity

of polystyrene obtained via MD simulations. However, in their studies, pressures up to

only 60 MPa were investigated, and consequently no dependence on the elastic constants

was determined.

A structural model of amorphous atactic polystyrene (PS) including all atoms was

initially generated by a Monte-Carlo algorithm based on the rotational isomeric state (RIS)

11

model [36]. The initial structure was then equilibrated at T=298 K and various hydrostatic

pressures for times up to 3 ns until a stable density was reached. The model contained

6084 atoms in 18 chains, packed in a bar-shaped cell. At ambient pressure, the size of the

simulation cell was 139.6×22.5×21.4 $\mathrm{\AA}^3$, corresponding to a density of 0.966 g cm^{-3}. At a

pressure of 20 GPa, the stable density was 1.665 g cm^{-3}.

To calculate the thermal conductivity, we used an MD time step of 0.5 fs and periodic

boundary conditions in 3 dimensions. The temperature and pressure were controlled

during equilibration by a Berendsen thermostat and barostat. The non-equilibrium

thermal conductivity [37] was determined using a constant heat flux imposed by a heat

source at the center of the computational cell and a heat sink at the edges of the cell. The

value of the flux was chosen such that the total temperature drop across the model was in

the range of 20-50 K. In steady-state, a linear temperature profile is established and the

thermal conductivity was evaluated from Fourier's law. Molecular dynamics simulations

capture heat transfer due to propagating (polarized), and diffusive (delocalized but not

polarized) modes, as well as heat transfer between localized modes when anharmonic

effects are important [7-9]. By analyzing the results as a function of cell size, we

established that the conductivity converges at cell sizes of approximately 10 nm. Our

reported results are for a simulation cell that is 14 nm long at ambient pressure.

Figure 3 presents the pressure dependence of the thermal conductivity of polystyrene by MD simulations. The solid line shows the predicted Λ based on the minimum thermal conductivity model with $\Lambda_0 = 5.66 \times 10^{-11}$ $J^{1/2}$ m $K^{-1}s^{-1}$, determined from a fit to $\Lambda_{min} = 0.20$ W m^{-1} K^{-1} at ambient pressure. The excellent agreement between the MD simulations and the model prediction indicates that the mechanism of thermal transport in amorphous polymers is the same as assumed by the minimum thermal conductivity model. It also suggests that indeed a universal thermal transport mechanism exists in amorphous polymers where thermal energy is transferred predominately through the diffusion of thermal energy between non-propagating vibrational modes.

As a striking contrast with the relatively weak pressure dependence predicted by the model of minimum thermal conductivity, the Leibfried-Schlömann (LS) equation, often used to describe the thermal conductivity of isotropic crystalline solids, predicts a strong pressure dependence:

$$\Lambda_{LS} = A \frac{V^{\frac{1}{3}} \omega_D{}^3}{\gamma^2 T}, \qquad (1)$$

where V is the volume, ω_D the Debye frequency, γ the Grüneisen constant, T the temperature, and A is a constant independent of pressure [38, 39]. If we assume that γ is also independent of pressure and $\omega_D \propto \sqrt{C_{11}}$, then the predicted $\Lambda(P)$ based on Eq. (1) is

shown as the dashed line in Fig. 3. The distinctly different pressure dependence of Λ predicted by the LS equation supports our conclusion that diffusion of thermal energy between non-propagating vibrational modes dominates heat conduction in amorphous polymers. The propagation of wave-like vibrational modes—the dominant heat conduction mechanism in crystalline structures—is a minor consideration.

IV. CONCLUSION

In summary, we have studied the pressure dependence of elastic constants and thermal conductivity of PMMA using time-domain Brillouin scattering and time-domain thermoreflectance combined with SiC anvil cell techniques. The pressure dependent $\Lambda(P)$ of PMMA by TDTR measurements and polystyrene by MD simulations can both be well accounted for by the model of minimum thermal conductivity. It also appears that there is no need to invoke localized excitations and non-harmonic energy transfer to capture the basic heat transfer mechanism in amorphous polymers. We point out, however, that with increasing pressure, contrast in the bonding strength between non-bonded and covalent interactions becomes less pronounced; these effects may reduce the density of localized vibrations at high pressures and suppress contributions to thermal transport from localized modes and anharmonic effects.
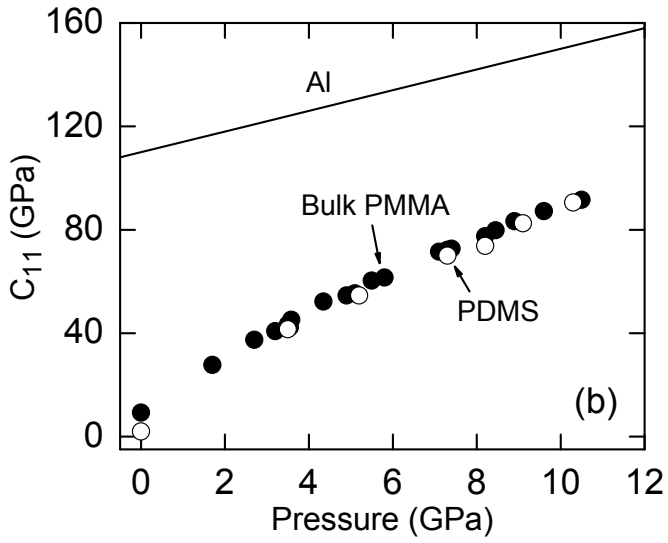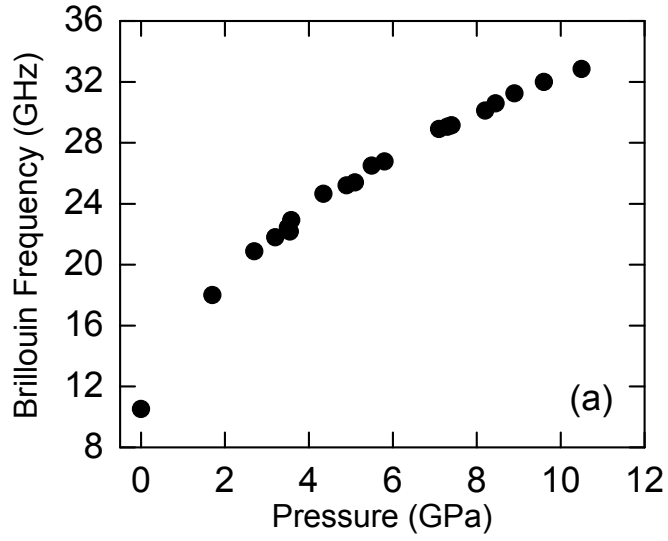
ACKNOWLEDGMENTS

FIG. 1. Pressure dependence of the (a) Brillouin frequency and (b) C_{11} of a spun-cast layer

of PMMA. C_{11} is derived from the Brillouin frequency data using a self-consistent

equation of state of PMMA and the assumptions that the Poisson ratio is constant and the

refractive index follows the Lorentz-Lorenz equation. Data for PDMS [40] and

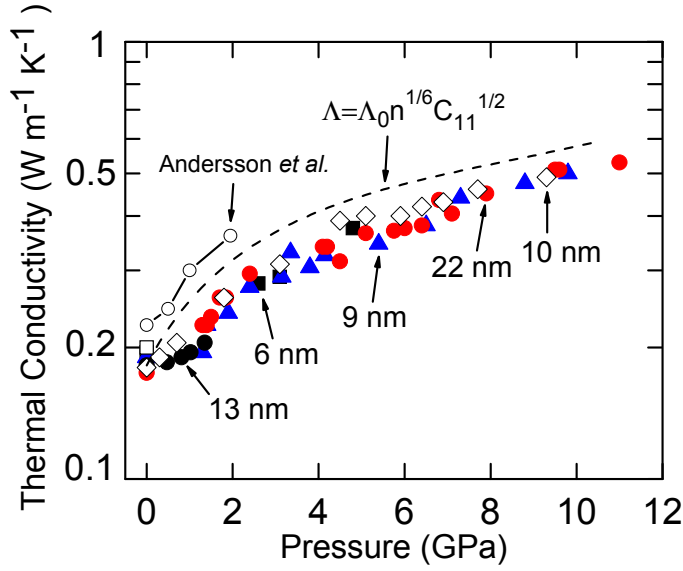previously estimated $C_{11}= 110$ GPa$+4P$ of Al [41] are plotted for comparison.

FIG. 2. Measurements of the thermal conductivity of PMMA brushes (solid symbols) and

a spun-cast layer (open diamond) as a function of pressure. The uncertainty in the thermal

conductivity and pressure measurements are ≈10 % and 0.2 GPa, respectively. Ar was the

pressure medium for all measurements except for that of 13 nm brushes and 10 nm

spun-cast layer where H_2O was used. The dashed line shows the predicted thermal

conductivity of PMMA based on the minimum thermal conductivity model, the pressure

dependence of the atomic density n, and the elastic constant C_{11} obtained by a polynomial

fit. Data for bulk PMMA by Andersson *et al.* (open circle) [10] and by Cahill *et al.* and

Putnam *et al.* (open square) [30, 31] are included for comparison. Lines between

Andersson's data are added to emphasize that the pressure dependence of the prior data

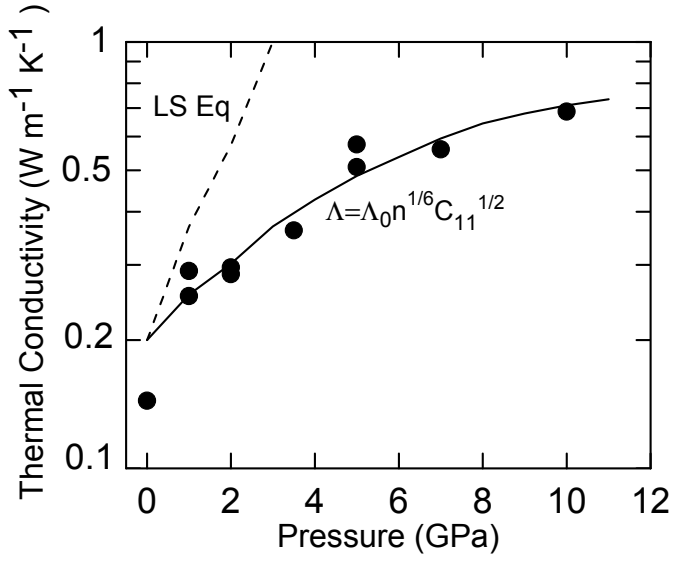are similar to that of our measurements in the low pressure regime.

FIG. 3. Pressure dependence of the thermal conductivity of polystyrene by molecular dynamics simulations (solid circles). The solid line shows the predicted thermal conductivity by the model of the minimum thermal conductivity. The pressure dependence of the thermal conductivity predicted by the Leibfried-Schlömann equation using the scaling $\omega_D \propto \sqrt{C_{11}}$ is shown as the dashed line.

*whsieh2@illinois.edu

[1] A. Einstein, Ann. Phys. **35**, 679 (1911).

[2] D. G. Cahill, S. K. Watson, and R. O. Pohl, Phys. Rev. B **46**, 6131 (1992).

[3] P. B. Allen, and J. L. Feldman, Phys. Rev. B **48**, 12581 (1993).

[4] P. B. Allen, J. L. Feldman, J. Fabian, and F. Wooten, Philosophical Magazine B **79**, 1715 (1999).

[5] H. S. Yang, D. G. Cahill, X. Liu, J. L. Feldman, R. S. Crandall, B. A. Sperling, and J. R. Abelson, Phys. Rev. B **81**, 104203 (2010).

[6] S. Alexander, O. Entinwohlman, and R. Orbach, Phys. Rev. B **34**, 2726 (1986).

[7] S. Shenogin, A. Bodapati, P. Keblinski, and A. McGaughey, J. Appl. Phys. **105**, 034906 (2009).

[8] D. M. Leitner, Annu. Rev. Phys. Chem. **59**, 233 (2008).

[9] X. Yu, and D. M. Leitner, J. Chem. Phys. **122**, 054902 (2005).

[10] S. P. Andersson, and R. G. Ross, International J. of Thermophys. **15**, 949 (1994).

[11] R. E. Barker, R. Y. S. Chen, and R. S. Frost, J. Polymer Sci. B **15**, 1199 (1977).

[12] R. S. Frost, R. Y. S. Chen, and R. E. Barker, J. Appl. Phys. **46**, 4506 (1975).

[13] E. H. Abramson, J. M. Brown, and L. J. Slutsky, J. Chem. Phys. **115**, 10461 (2001).

[14] P. Beck, A. Goncharov, V. V. Struzhkin, B. Militzer, H. K. Mao, and R. J. Hemley, Appl. Phys. Lett. **91**, 181914 (2007).

[15] W. P. Hsieh, B. Chen, J. Li, P. Keblinski, and D. G. Cahill, Phys. Rev. B **80**, 180302 (2009).

[16] S. Boyes, A. M. Granville, and W. J. Brittain, Macromolecular Synthesis **13**, 15 (2004).

[17] C. B. Gorman, R. J. Petrie, and J. Genzer, Macromolecules **41**, 4856 (2008).

[18] Y. Tsujii, K. Ohno, S. Yamamoto, A. Goto, and T. Fukuda, Adv Polym Sci **197**, 1 (2006).

[19] C. Thomsen, H. T. Grahn, H. J. Maris, and J. Tauc, Phys. Rev. B **34**, 4129 (1986).

[20] J. Wittlinger, R. Fischer, S. Werner, J. Schneider, and H. Schulz, Acta Cryst. B **53**, 745 (1997).

[21] H. K. Mao, P. M. Bell, J. W. Shaner, and D. J. Steinberg, J. Appl. Phys. **49**, 3276 (1978).

[22] D. G. Cahill, W. K. Ford, K. E. Goodson, G. D. Mahan, A. Majumdar, H. J. Maris, R. Merlin, and S. R. Phillpot, J. Appl. Phys. **93**, 793 (2003).

[23] C. A. Paddock, and G. L. Eesley, J. Appl. Phys. **60**, 285 (1986).

[24] D. A. Young, C. Thomsen, H. T. Grahn, H. J. Maris, and J. Tauc, in *Phonon Scattering in Condensed Matter*, edited by A. C. Anderson and J. P. Wolfe (Springer, Berlin, 1986).

[25] D. G. Cahill, Rev. Sci. Instrum. **75**, 5119 (2004).

[26] Z. B. Ge, D. G. Cahill, and P. V. Braun, Phys. Rev. Lett. **96**, 186101 (2006).

[27] K. E. O'Hara, X. Y. Hu, and D. G. Cahill, J. Appl. Phys. **90**, 4852 (2001).

[28] C. Thomsen, H. T. Grahn, H. J. Maris, and J. Tauc, Opt. Commun. **60**, 55 (1986).

[29] S. Rabinowitz, I. M. Ward, and J. S. C. Parry, J Mater Sci **5**, 29 (1970).

[30] D. G. Cahill, and R. O. Pohl, Phys. Rev. B **35**, 4067 (1987).

[31] S. A. Putnam, D. G. Cahill, B. J. Ash, and L. S. Schadler, J. Appl. Phys. **94**, 6785 (2003).

[32] M. D. Losego, L. Moh, K. A. Arpin, D. G. Cahill, and P. V. Braun, Appl. Phys. Lett. **97**, 011908 (2010).

[33] J. L. Feldman, M. D. Kluge, P. B. Allen, and F. Wooten, Phys. Rev. B **48**, 12589 (1993).

[34] H. Sun, J. Comput. Chem. **15**, 752 (1994).

[35] E. A. Algaer, M. Alaghemandi, M. C. Bohm, and F. Muller-Plathe, J. Phys. Chem. A **113**, 11487 (2009).

[36] M. Rehahn, W. L. Mattice, and U. W. Suter, Adv. Polym. Sci. **131-132**, 460 (1997).

[37] P. K. Schelling, S. R. Phillpot, and P. Keblinski, Phys. Rev. B **65**, 144306 (2002).

[38] G. A. Slack, in *Solid State Physics* (Academic, New York, 1979) **34**, 35.

[39] M. Roufosse, and P. G. Klemens, Phys. Rev. B **7**, 5379 (1973).

[40] L. L. Stevens, E. B. Orler, D. M. Dattelbaum, M. Ahart, and R. J. Hemley, J. Chem. Phys. **127**, 104906 (2007).

[41] C. Bercegeay, and S. Bernard, Phys. Rev. B **72**, 214101 (2005).